Reaction of Fluorine Atoms with Monomeric and Polymeric Uranium Pentafluoride

John L. Lyman* and Redus Holland

Chemistry Division, Los Alamos National Laboratory, Los Alamos, New Mexico 87545
(Received: January 5, 1987; In Final Form: April 6, 1987)

We have measured the room-temperature rate constants for formation of UF_6 from the reaction of fluorine atoms with UF_5. The rapid growth of UF_5 clusters (polymers) from the nascent monomeric species complicates the rate measurements. The ratio of the rate of UF_5-dimer formation to the rate of monomer–fluorine recombination is insensitive to the cluster formation. That ratio, $k_{mm}/k_{rm} = 5.0 \pm 1.0$, is our most reliable experimental result. It, along with additional experimental data, gives $k_{rm} = 8.0 \times 10^{-12}$ cm^3 molecule^{-1} s^{-1} and $k_{mm} = 4.0 \times 10^{-11}$ cm^3 molecule^{-1} s^{-1}. To obtain the dependence of reaction rates on s, the average UF_5 polymer size, we assumed that the rates were proportional to the collision rate. The derived rate constants were $k_{pp} = k_{mm}s^{1/6}$ cm^3 molecule^{-1} s^{-1} for cluster growth and $k_{rp} = 4.1 \times 10^{-14}(1 + 2s^{1/3})^2$ cm^3 molecule^{-1} s^{-1} for reaction of fluorine atoms with polymeric UF_5. The experimental procedure was to photolyze both F_2 and UF_6 in helium diluent with a KrF excimer laser to produce UF_5 and an excess of fluorine atoms. This allowed the slower recombination reactions to compete with polymerization. We monitored the transient concentration of UF_6 with an ultraviolet probe beam at 215 nm. The recombination of fluorine atoms with UF_5 monomer is substantially faster than recombination with the polymer.

Introduction

The thermal and photochemical reactions of UF_6 produce the reactive species UF_5 and F. Knowledge of the mechanisms and rates for production and reaction of these species is essential for understanding any application involving UF_6 at high temperatures or photolysis of UF_6. The most widely investigated application has been uranium isotope separation by laser and by other methods.

The main reactions of interest in this study are the recombination of fluorine atoms with UF_5 monomer or polymer

$$F + (UF_5)_n \rightarrow (UF_5)_{n-1} + UF_6 \qquad n > 0 \qquad (1)$$

and the polymerization of UF_5

$$(UF_5)_m + (UF_5)_n \rightarrow (UF_5)_{m+n} \qquad m, n > 0 \qquad (2)$$

The measurement of the rates of these reactions is particularly difficult because of the rapid growth of UF_5 polymers during the time of the reaction observation.

Because reaction 2 is so much faster than reaction 1 when only UF_6 is photolyzed, the earlier[1] investigation of these reactions gave only an upper limit for the rate constant of recombination of fluorine atoms with UF_5 (reaction 1) of

$$k_r < 2.0 \times 10^{-12} \text{ cm}^3 \text{ molecule}^{-1} \text{ s}^{-1} \qquad (3)$$

These experiments did not detect any recombination and, therefore, did not distinguish between recombination with monomeric and polymeric UF_5.

The experiments reported in the present paper allowed us to see reaction 1. We accomplished this by photolyzing molecular fluorine along with UF_6. This increased the initial ratio of F to UF_5, and thus accelerated reaction 1 relative to reaction 2.

That earlier study[1] gave the rate constant

$$k_{mm} = (1.0 \pm 0.2) \times 10^{-11} \text{ cm}^3 \text{ molecule}^{-1} \text{ s}^{-1} \qquad (4)$$

for the monomer–monomer reaction (reaction 2, $m = n = 1$). For reactions involving polymers the authors assumed that the rate constant was proportional to the collision rate.

Other papers[2,3] also reported rate constants for the monomeric forms of reactions 1 and 2. The rate constants of ref 2 were based on insufficiently precise data, and those of ref 3 were derived from experiments dominated by thermal expansion and diffusion. Reference 1 discusses these experiments in greater detail.

The improved experimental technique in the present paper showed that reaction 1 is much faster for monomeric UF_5 than for polymeric UF_5. Our observations also resulted in a revision of the rate of reaction 2.

Experimental Section

The experimental technique was to photodissociate UF_6 and F_2 and to monitor the subsequent concentration of UF_6 by UV absorption. Figure 1 shows the optical arrangement for the experiments. Photolysis produces the reactive species UF_5 and F.

The photolysis cell body was made of nickel. Sapphire windows were bonded by nickel-plated kovar sleeves to monel flanges. The windows were tilted 5° to prevent interference from reflected beams. The cell length was 17 cm and the volume was 345 cm^3. The construction of the cell was such that heating was possible up to about 700 K, but all results in this paper were at room temperature (295 K).

The gas mixtures were prepared in a stainless-steel vessel and allowed to sit for several hours before transfer to the photolysis cell. The uranium hexafluoride and fluorine were synthesized at Los Alamos. All other gases were from commercial sources and were used without further purification.

Most commercial fluorine has a high oxygen impurity. This was intolerable for these experiments. Our method of monitoring the UF_6 concentration was to use an ultraviolet (deuterium) lamp and to measure the time response of the absorption by the photolyzed gas sample at 215 nm. At that wavelength O_2F produced by the reaction[4]

$$O_2 + F + M \rightarrow O_2F + M \qquad (5)$$

absorbs strongly and interferes with the measurement of the UF_6 concentration. We solved this problem by using high purity fluorine prepared by L. B. Asprey[5] of Los Alamos National Laboratory.

The lamp and lenses (Figure 1) provided a nearly parallel beam of UV light that was entirely within the region of the photolyzed sample. The dielectric mirrors allowed for counterpropagation of the two beams and prevented laser damage of the deuterium lamp. The electronic shutter prolonged the life of the photomultiplier. It opened a few milliseconds prior to the laser pulse. A Tektronix 7612D transient digitizer processed the photomultiplier signal, which was in turn stored in a computer for later analysis.

The KrF excimer laser produced up to 600 mJ/pulse with an area at the photolysis cell of 3.0 cm^2. The UV probe beam area was about 0.25 cm^2. The laser pulse energy was reproducible to within about 3%. The transmittance of the first two mirrors and

(1) Lyman, J. L.; Laguna, G.; Greiner, N. R. *J. Chem. Phys.* **1985**, *82*, 175.
(2) Lewis, W. B.; Wampler, F. B.; Huber, E. J.; Fitzgibbon, G. C. *J. Photochem.* **1979**, *11*, 393.
(3) Kim, K. C.; Reisfeld, M.; Seitz, D. *J. Chem. Phys.* **1980**, *73*, 5605.
(4) Matchuk, N. M.; Tupikow, V. I.; Malkova, A. I.; Pshezhetskii, S. Ya. *Opt. Spectrosc.* **1976**, *40*, 7.
(5) Asprey, L. B. *J. Fluorine Chem.* **1976**, *7*, 359.

0022-3654/87/2091-4821$01.50/0

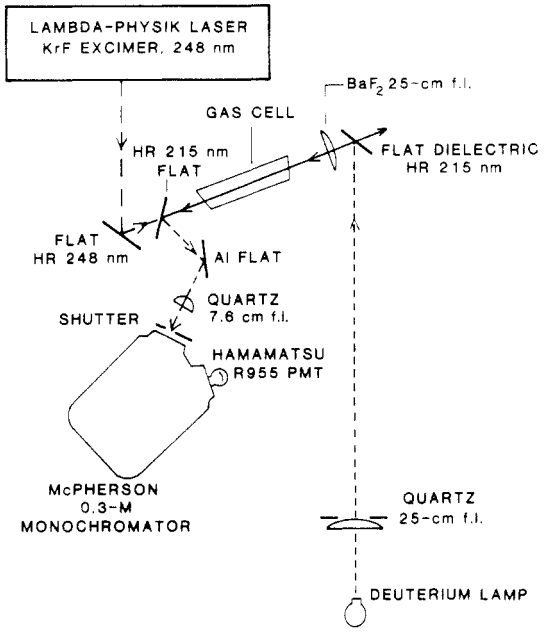

Figure 1. Schematic diagram of the optical arrangement in the photolysis experiments.

the cell entrance window was 0.59.

A typical experiment consisted of measuring the pulse energy at the laser exit (E), the UV signal with the cell empty (S_0), the UV signal with the cell loaded (S), and the UV transient deviation from that signal ($\Delta S(t)$). The time scale of the transient measurements ranged from 100 μs to 35 ms. For the short measurements the photomultiplier detected scattered light from the laser pulse and luminescence from the irradiated gas during the first 10 μs. We attempted to correct for this effect by subtracting a waveform with the UV lamp blocked. However, some uncertainty still remains during the first few microseconds of the transient signal.

For most experiments we used fresh gas samples with only one laser pulse. We found that UF_5 particles from previous pulses absorbed to some extent at both the photolysis and probe frequencies. However, this effect was nearly nonexistent at high fluorine concentrations, and we did do some averaging of signals from multiple laser pulses on a single filling in some cases.

Data Reduction

The intent in these experiments was to use the initial gas composition, measured absorption cross sections, and measured pulse energies to determine the concentration of all species immediately after the laser pulse. The second step was to use the transient absorption signal to monitor the UF_6 concentration after the laser pulse. The final step was to determine the appropriate rate constants from the observed transient behavior of the UF_6 concentration.

The fraction of each species that the laser pulse dissociates depends on the laser fluence, Φ. The average laser fluence[6] in the irradiated region of the photolysis cell is

$$\Phi = (ET_w/A)(T_L - 1)/\ln T_L \quad (6)$$

where E is the pulse energy, T_w is the transmittance of the mirrors and windows between the laser and the gas sample, A is the beam area, and T_L is the laser transmittance of the gas sample. The quantity T_L is calculated from the gas composition, the cell length, and the absorption cross sections at 248 nm. The absorbing species in the initial gas composition are UF_6 and F_2. The laser transmittance is therefore

$$T_L = \exp(-(\sigma_u(248)[UF_6] + \sigma_f(248)[F_2])L) \quad (7)$$

(6) Lyman, J. L.; Quigley, G. P.; Judd, O. P. In *Multiple-Photon Excitation and Dissociation of Polyatomic Molecules*, Cantrell, C. D., Ed.; Springer-Verlag: Heidelberg, 1986; pp 9–122.

TABLE I: Absorption Cross Sections at Laser and Probe Wavelengths

species	wavelength, nm	cross section, cm^2	ref
UF_6	248	1.6×10^{-18}	7
UF_6	215	1.8×10^{-17}	7
F_2	248	1.43×10^{-20}	8[a]
F_2	215	3.6×10^{-21}	b,c
UF_5	215	4.3×10^{-18} [d]	b

[a] Confirmed by independent measurement. [b] Inferred from experiment. [c] Reference 8 has a slightly higher value. [d] Assumed $\sigma((UF_5)_n) = n\sigma(UF_5)$.

where $\sigma_u(248)$ and $\sigma_f(248)$ are the cross sections at 248 nm, the u and f refer to UF_6 and F_2, respectively, and L is the path length.

For UF_6 the fraction dissociated is

$$f_u = 1 - \exp(-\sigma_u(248)\Phi/h\nu) \quad (8)$$

and for F_2

$$f_f = 1 - \exp(-\sigma_f(248)\Phi/h\nu) \quad (9)$$

The species that absorb the 215-nm probe beam all reduce the probe transmittance. While UF_6 is the dominant absorber, the species F_2 and UF_5 each absorb at that wavelength. The expression for the probe transmittance is

$$T_p = \exp(-(\sigma_u(215)[UF_6] + \sigma_f(215)[F_2] + \sigma_5(215)[UF_5])L) \quad (10)$$

where the absorption cross sections are for 215 nm and the subscript "5" refers to UF_5. The probe transmittance prior to the laser pulse is just S/S_0, and after the laser pulse it is

$$T_p = (S + \Delta S(t))/S_0 \quad (11)$$

Because of some reaction losses of UF_6 during preparation, storage, and transport of the gas mixtures, we use the probe transmittance and eq 10 to determine the initial UF_6 concentration. Equations 10 and 11 give the concentration of UF_6 as chemical reactions alter it after the laser pulse. Independent experiments with no F_2 and with methane to prevent re-formation of UF_6 gave the UF_5 absorption cross section at 215 nm.

Table I lists the appropriate absorption cross sections for species involved in the experiment.

For a mixture of UF_6, F_2, and He, the densities of the different species immediately after the laser pulse are

$$[F]_0 = [UF_6]_i f_u + 2[F_2]_i f_f \quad (12)$$

$$[UF_5]_0 = [UF_6]_i f_u \quad (13)$$

$$[UF_6]_0 = [UF_6]_i(1 - f_u) \quad (14)$$

$$[F_2]_0 = [F_2]_i(1 - f_f) \quad (15)$$

here the "0" subscript indicates after the laser pulse and the "i" subscript indicates before the pulse. Equations 8 and 9 define f_u and f_f.

Results

The transient absorption experiments gave signals like Figure 2. This particular experiment was with a 1000-Torr sample of 1% CH_4 and 0.02% UF_6 in helium diluent. The methane reacts rapidly[9] with fluorine atoms and, thus, prevents recombination to UF_6. Furthermore, the methyl radical that this reaction produces does not react significantly[10] with UF_6. The experiments with methane allow a measurement of the UF_5 absorption cross section without the complication of recombination and other reactions that deplete or produce absorbing molecules.

Note that the transmitted signal increases promptly at the laser pulse and then remains nearly constant. One reaction that does occur during this period is polymerization of UF_5. The near constant signal level after the laser pulse indicates that the ab-

(7) DePoorter, G. L.; Rofer-DePoorter, C. K. *Spectrosc. Lett.* **1975**, *8*, 521.
(8) Calvert, J. G.; Pitts, J. N. *Photochemistry*; Wiley: New York, 1966; p 184.
(9) Jones, W. E.; Skolnic, E. G. *Chem. Rev.* **1976**, *76*, 563.
(10) Lyman, J. L.; Laguna, G. *J. Chem. Phys.* **1985**, *82*, 183.

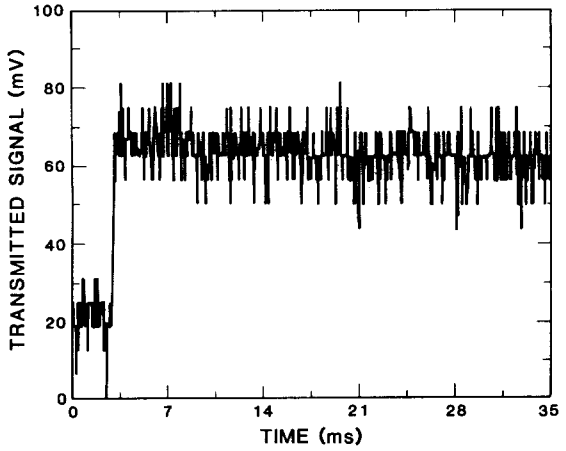

Figure 2. Digitized transmitted signal for a gas mixture consisting of 0.02% UF_6, 1.0% CH_4, with He diluent at 1000 Torr total pressure. The laser pulse, energy 0.49 J, dissociated 16.5% of the UF_6 in the optical path.

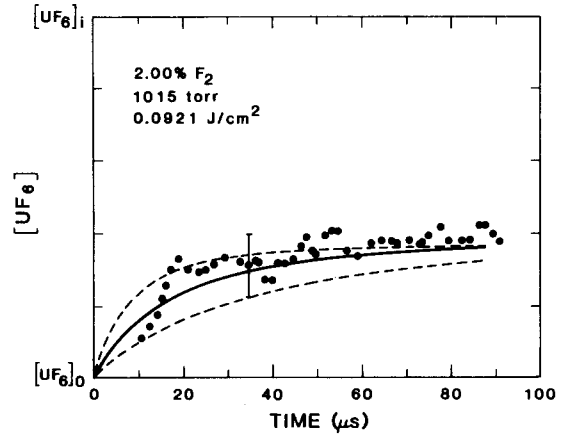

Figure 3. UF_6 concentration vs. time, $[UF_6]_i = 5.4 \times 10^{15}$ molecule/cm^3, $f_u = 0.168$, points are experimental, the solid curve is the model calculation for the rate constants given in a later section, and the dashed curves are for $k_{mm} = 2$ and 6×10^{-11} cm^3 molecule^{-1} s^{-1} with $k_{mm}/k_{rm} = 5.0$.

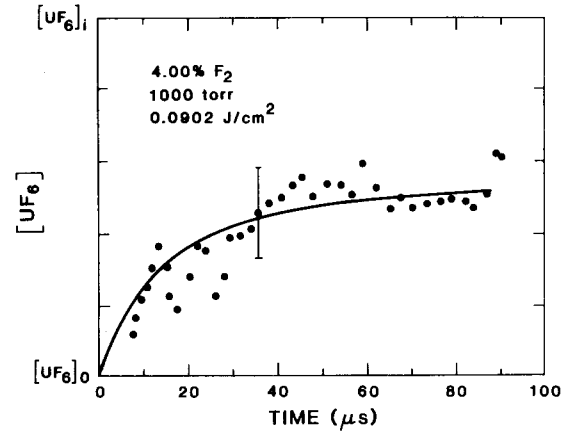

Figure 4. UF_6 concentration vs. time, $[UF_6]_i = 5.6 \times 10^{15}$ molecule/cm^3, $f_u = 0.165$. The solid curve is the model calculation.

sorption cross section per UF_5 unit changes very little with polymer size. In the data analysis we assumed no variation in the cross section with polymer size.

In all experiments without methane present the transmitted signal decreases with time after the laser pulse. We converted the transient signals to UF_6 concentration vs. time. Figures 3–9 show results for UF_6 with varying amounts of F_2. In these figures the points were taken from the transient signals (like Figure 2). The figures also show as lines the results of model calculations that we discuss below. The error bar in each figure represents

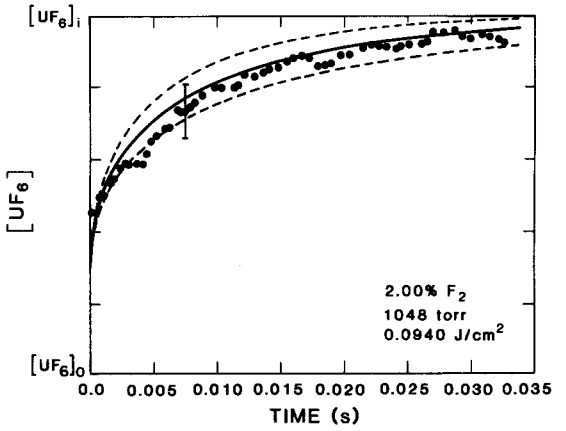

Figure 5. UF_6 concentration vs. time, $[UF_6]_i = 5.6 \times 10^{15}$ molecule/cm^3, $f_u = 0.171$. The solid curve is the model calculation. The upper dashed curve is for k_{rp} increased 22% and the lower for a 19% reduction in k_{rp}.

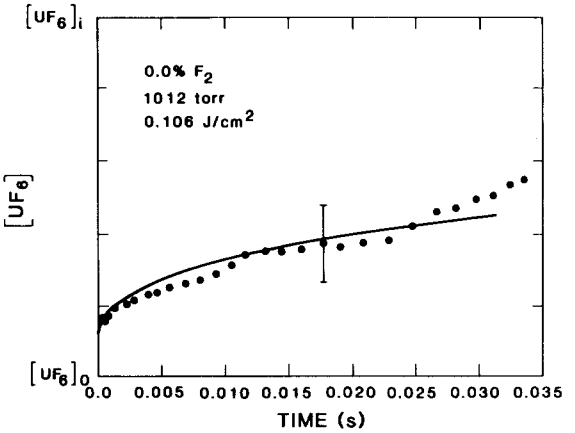

Figure 6. UF_6 concentration vs. time, $[UF_6]_i = 5.1 \times 10^{15}$ molecule/cm^3, $f_u = 0.191$. The solid curve is the model calculation.

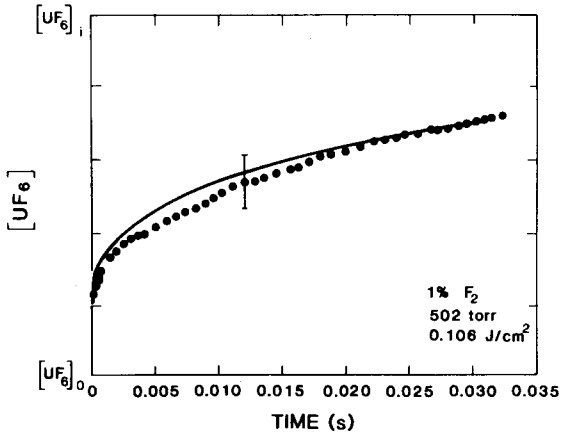

Figure 7. UF_6 concentration vs. time, $[UF_6]_i = 2.6 \times 10^{15}$ molecule/cm^3, $f_u = 0.191$. The solid curve is the model calculation.

the signal noise. The top of the graph in each figure is $[UF_6]_i$, and the bottom is $[UF_6]_0$ (eq 14). As outlined in the previous section, the experimental conditions (pressure, UF_6 fraction, pulse energy) give these two values, and the transient signals show how the UF_6 concentration varies between $[UF_6]_0$ and $[UF_6]_i$.

The UF_6 concentration initially rises rapidly and then tends to plateau and rise at a much slower rate (Figures 3–9). We only see the initial rise of the UF_6 in the short time scans (Figures 3 and 4). The point of the plateau we define as

$$Y = -\ln [(S + \Delta S(t))/S_0] + \ln [(S + \Delta S(0))/S_0] = ([UF_6]_i - [UF_6]_{0.2})/([UF_6]_i - [UF_6]_0) \quad (16)$$

or the deviation of the UF_6 concentration from the $[UF_6]_i$ at about 0.2 ms divided by the deviation at the laser pulse. Y is the fraction

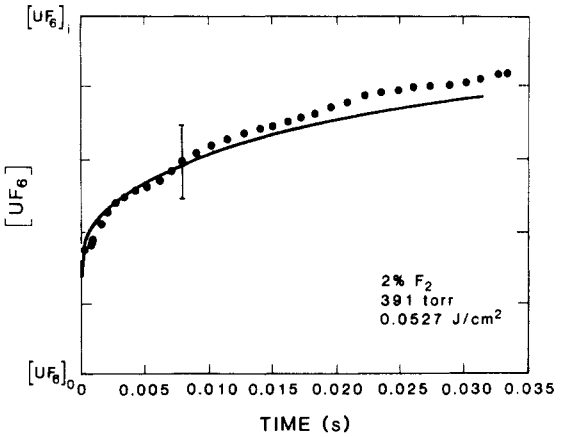

Figure 8. UF_6 concentration vs. time, $[UF_6]_i = 1.8 \times 10^{15}$ molecule/cm^3, $f_u = 0.100$. The solid curve is the model calculation.

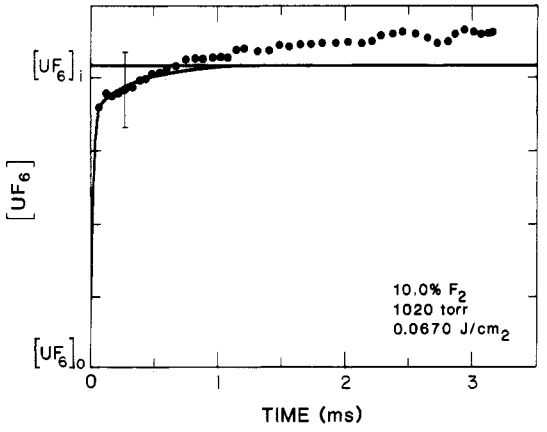

Figure 9. UF_6 concentration vs. time, $[UF_6]_i = 2.3 \times 10^{15}$ molecule/cm^3, $f_u = 0.125$. The solid curve is the model calculation.

of the UF_5 produced which is present as polymers after most of monomer has disappeared.

Mechanism, Model, and Rate Constant Determination

The UV laser pulse dissociates both UF_6

$$UF_6 \xrightarrow{h\nu} UF_5 + F \tag{17}$$

and F_2

$$F_2 \xrightarrow{h\nu} 2F \tag{18}$$

The first reactions that may occur at reaction 1 with $n = 1$ and reaction 2 with $m = n = 1$. With the accumulation of UF_5 dimers and higher polymers the reactions 1 and 2 may occur with $n > 1$.

We do not need to consider the breakup of UF_5 clusters (the reverse of reaction 2) at room temperature. The UF_5 moieties are tightly bound. The enthalpy changes[11] for UF_5-dimer bond cleavage and for vaporization of UF_5 from the solid material are respectively 40.0 and 39.0 kcal/mol.

The rate constant designations for recombination (reaction 1) and polymerization (reaction 2) are the following:

k_{rm}	reaction 1 with $n = 1$
k_{rp}	reaction 1 with $n > 1$
k_{mm}	reaction 2 with $m = n = 1$
k_{mp}	reaction 2 with $m = 1$, $n > 1$
k_{pp}	reaction 2 with m, $n > 1$

In this section we obtain values for each of these rate constants and clarify the reaction mechanism. Because of the complexity of the reactions, we employ a simple reaction model. Our procedure is not, however, simply to adjust a set of parameters to the experimental data, but to choose experimental conditions rationally such that only a small set of constants are sensitive to a given experimental result. We first make some simplifying assumptions about the rates of reaction with polymeric UF_5. We then derive the ratio k_{mm}/k_{rm} from the change of Y (eq 16) with fluorine concentration. The value of k_{rm} and k_{mm} then follows directly from the initial rapid signal rise. The values of k_{mp} and k_{pp} are tied directly to k_{mm} by the simplifying assumptions. The final constant, k_{rp}, is then obtained by fitting the slower signal rise at longer time.

Effect of Polymer Size on Reaction Rates. Reactions 1 and 2 change the average particle size, s, or the average number of UF_5 units per particle. That size is

$$s = \sum_n n[UF_5]_n / \sum_n [UF_5]_n \tag{19}$$

the numerator is the total concentration of UF_5 in any polymeric form. The denominator is the concentration of UF_5 polymeric particles.

In the absence of information about the effect of UF_5 polymer size on the rates of reactions 1 and 2, we assume the rates to be proportional to the collision rate for the average polymer size. To estimate the collision rate we assume that polymerization produces close-packed spheres. The particle volume is, therefore, proportional to the molecular size, s. The cross section is then proportional to $s^{2/3}$, and the velocity to $s^{-1/2}$. These assumptions give

$$k_{pp} \propto s^{1/6} \tag{20}$$

$$k_{mp} \propto (1 + s^{1/3})^2(1 + s^{-1})^{1/2} \tag{21}$$

$$k_{rp} \propto (1 + 2s^{1/3})^2 \tag{22}$$

The latter expression is only approximate. It assumes that the collision diameter of UF_5 monomer is twice that of the fluorine atom.

Determination of k_{mm}/k_{rm}. The experimental results suggest that some reaction initially produces UF_6 at a rapid rate and that a slower reaction produces some UF_6 at later times. We propose that the rapid rise in the UV absorption is due to reaction 1 with $n = 1$, and that the much slower rise at longer times is due to reaction 1 with $n > 1$. We correlate the consumption of UF_5 monomer with the end of the rapid rise of UF_6 concentration.

At early times reactions 1 and 2 compete for the available monomeric UF_5, but only reaction 1 produces UF_6. Therefore, the amount of UF_6 produced at the time of consumption of the monomeric UF_5 depends on the relative rates of the monomeric forms of reactions 1 and 2. A high $[F]_0/[UF_5]_0$ ratio favors reaction 1, and a low ratio favors reaction 2. (The quantity Y is the fraction of the dissociated UF_6 that has *not* recombined to UF_6 at the time of consumption of the UF_5 monomer.)

The graph of Y vs. $[F]_0/[UF_5]_0$ (Figure 10) is a sensitive measure of the rate constant ratio k_{mm}/k_{rm}. The points were taken from the experiments (Figures 3–9 and similar data), and the curves were taken from Figure 11 and similar calculations with different values of the ratio k_{mm}/k_{rm}. The best fit (solid curve) in Figure 10 is for a rate-constant ratio of

$$k_{mm}/k_{rm} = 5.0 \tag{23}$$

The data scatter gives a ±20% precision for this ratio. The quantity Y is insensitive to the individual values of the two rate constants and to the rate constant k_{rp}.

Reaction Model. One reaction that may influence the reaction mechanism is the recombination of fluorine atoms to molecules

$$F + F + M \xrightarrow{k_{ff}} F_2 + M \tag{24}$$

This reaction is too slow[9] to have a major influence on these experiments. Its rate constant[9] is

$$k_{ff} = 8.0 \times 10^{-35} \text{ cm}^6 \text{ molecule}^{-2} \text{ s}^{-1} \tag{25}$$

(11) Kleinschmidt, P. D.; Hildenbrand, D. L. *J. Chem. Phys.* **1979**, *71*, 196.

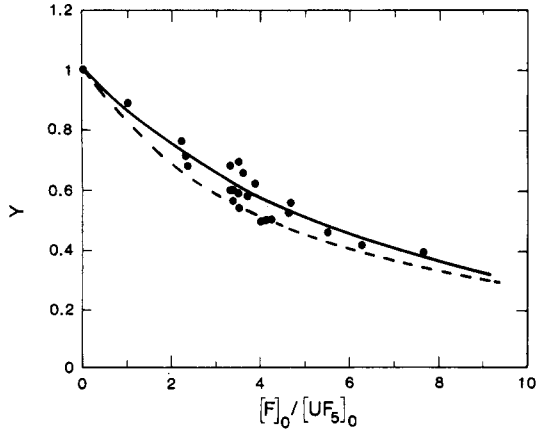

Figure 10. Experimental and calculated graphs of Y (eq 16) vs. $[F]_0/[UF_5]_0$. The solid curve is the model calculation for $k_{mm}/k_{rm} = 5.0$ and the dashed is for $k_{mm}/k_{rm} = 3.6$.

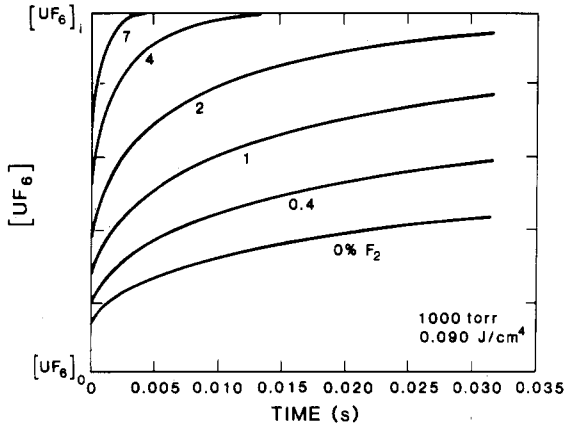

Figure 11. Calculated UF_6 concentration vs. time, $[UF_6]_i = 5.5 \times 10^{15}$ molecule/cm^3, $f_u = 0.165$. The curves are for 0, 0.4, 1, 2, 4, and 7% F_2.

From the features of the mechanism discussed we construct a model based on reactions 1, 2, and 24. The differential equations become

$$d[F]/dt = -k_{rm}[F][(UF_5)_1] - k_{rp}[F][(UF_5)_s] - 2k_{ff}[F]^2[M] \quad (26)$$

$$d[(UF_5)_1]/dt = -2k_{mm}[(UF_5)_1]^2 - k_{mp}[(UF_5)_1][(UF_5)_s] + \delta k_{rp}[F][(UF_5)_s] - k_{rm}[F][(UF_5)_1] \quad (27)$$

$$d[(UF_5)_s]/dt = k_{mm}[(UF_5)_1]^2 - \delta k_{rp}[F][(UF_5)_s] - k_{pp}[(UF_5)_s]^2 \quad (28)$$

$$d[UF_6] = k_{rm}[F][(UF_5)_1] + k_{rp}[F][(UF_5)_s] \quad (29)$$

$$d[F_2]/dt = k_{ff}[F]^2[M] \quad (30)$$

where the "s" subscript indicates a polymer of mean size "s", the "1" indicates monomer, and δ is the fraction of the polymers that are dimers. By assuming a Poisson distribution of polymer sizes we obtain

$$\delta = \exp(-(s - 2)) \quad (31)$$

Note that we use the assumption of a Poisson distribution only to estimate the fraction of monomeric UF_5. Because the rates of polymer reactions have very little dependence on polymer size, our conclusions are very insensitive to the precise form of the distribution. We also include the additional restriction of conservation of uranium atoms

$$s = ([UF_6]_i - [UF_6] - [(UF_5)_1])/[(UF_5)_s] \quad (32)$$

We used this model to make all of the calculations discussed in this paper.

Figures 11 and 12 show the calculated effect of molecular fluorine on the recovery of UF_6 concentration after photolysis.

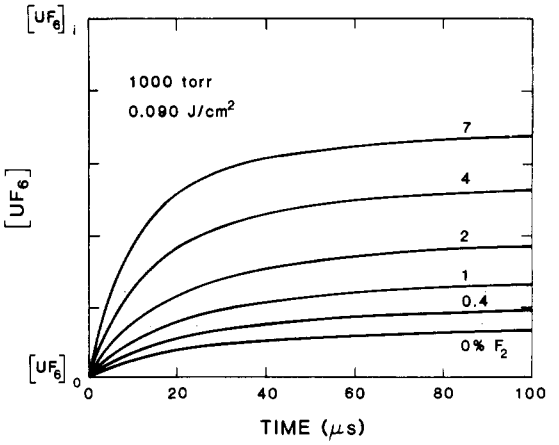

Figure 12. The first 100 microseconds of the calculations of Figure 11.

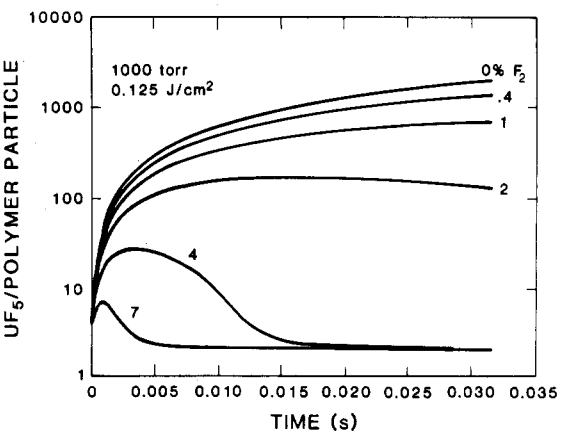

Figure 13. Average polymer sizes vs. time for the calculations of Figure 11. Note that the lower limit on S as defined is 2.

The figures are calculations of UF_6 concentration vs. time after photolysis for several different concentrations of molecular fluorine. As in Figures 3–9 the top of the figure is $[UF_6]_i$ and the bottom is $[UF_6]_0$. The amount of UF_5 produced by photolysis is the same for each curve, but the initial fluorine atom concentration increases with the percentage of molecular fluorine.

The time span for Figure 11 is 35 ms, which is the same as many of the experiments (Figures 5–9). Figure 12 is the same set of calculations for the first 0.1 ms. We see that the UF_6 concentration recovers very rapidly during the first few tens of microseconds followed by a much slower recovery. These calculations agree with the experiments. The solid curves in Figures 3–9 were calculated by the same method, but for the specific experimental conditions.

The calculations of Figures 11 and 12 also gave the increase of average particle size with time for different amounts of fluorine. Low fluorine concentrations give high rates of particle growth, and high concentrations give lower rates and an eventual decrease in particle size as the fluorine atoms consume the UF_5. Figure 13 shows the change of UF_5 polymer particle size with time for several initial concentrations of molecular fluorine.

Determination of Other Rate Constants. With the rate constant ratio in eq 23, the next step is the determination of the rate constant for dimerization of UF_5 (k_{mm}). This we do by comparison of the experiments at early times (Figures 3 and 4) with the model predictions. We see from Figure 3 that the best value is about 4×10^{-11} cm^3 molecule^{-1} s^{-1}. The precision for this rate constant is only about ±50%. The poor signal-to-noise ratio and the interference from light emission during the first ten microseconds both contribute to this uncertainty. The final adjustable parameter is the rate constant k_{rp} for recombination with the polymer. Comparison of the long-time experiments (Figures 5–9) with the model gives 4.1×10^{-14} cm^3 molecule^{-1} s^{-1} for the proportionality constant for eq 22. The precision is good for this value (Figure 5), but its value also depends on that of the other rate constants.

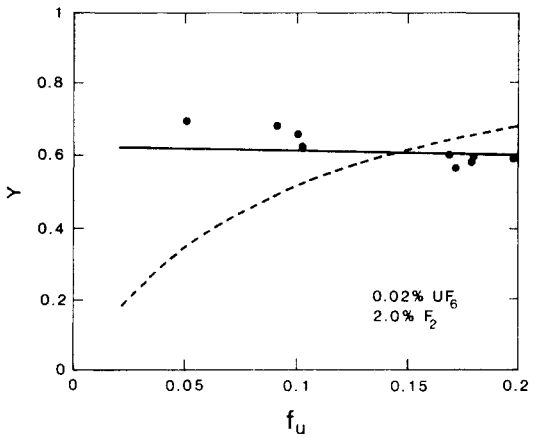

Figure 14. Experimental and calculated values of Y vs. f_u for 2% F_2, the solid curve is the model calculation, and the dashed curve assumes that all UF_6 re-forms by reaction 38.

In summary, comparison of the model with the experimental data gives

$$k_{rm} = 8.0 \times 10^{-12} \text{ cm}^3 \text{ molecule}^{-1} \text{ s}^{-1} \quad (33)$$

$$k_{mm} = 4.0 \times 10^{-11} \text{ cm}^3 \text{ molecule}^{-1} \text{ s}^{-1} \quad (34)$$

$$k_{rp} = 4.1 \times 10^{-14}(1 + 2s^{1/3})^2 \text{ cm}^3 \text{ molecule}^{-1} \text{ s}^{-1} \quad (35)$$

$$k_{mp} = k_{mm}\, 2^{-3/2}(1 + s^{1/3})^2(1 + s^{-1})^{1/2} \quad (36)$$

$$k_{pp} = k_{mm}s^{1/6} \quad (37)$$

Only the first three values involve adjustable parameters (eq 33–35). The others follow from the assumptions stated above.

We have shown that the experimental data are consistent with the proposed mechanism. However, one reaction that could possibly contribute to re-formation of UF_6 when molecular fluorine is present is

$$UF_5 + F_2 \rightarrow UF_6 + F \quad (38)$$

To show that this reaction does not contribute significantly to the experimental observations we measured the dependence of the ratio Y (eq 16) on the fraction f_u, and hence on $[UF_5]_0/[F_2]$ (Figure 14). All experiments were with 0.02% UF_6 and 2% F_2. The solid line is the prediction for mechanism proposed above, and the dashed curve is what one would expect if reaction 38 is the sole source of UF_6 after the laser pulse. The assumed rate constant for reaction 38 is 3×10^{-14} cm^3 molecule^{-1} s^{-1} for this calculation. We see that the original mechanism adequately reproduces the experiment and that reaction 38 cannot contribute more than a few percent to the recovery of UF_6. This allows us to set an upper limit for the rate constant for reaction 38 of 1×10^{-15} cm^3 molecule^{-1} s^{-1}.

Discussion

The most significant result of these experiments is that the rate of reaction of fluorine atoms with UF_5 monomer is substantially faster than the rate of reaction with UF_5 polymer. One reason for this difference is probably that the reaction with the monomer is a simple recombination reaction, while the polymer reaction requires formation of UF_6 in addition to release of that species from the polymeric cluster. The addition of the molecular fluorine to the gas mixture made possible the measurement of the fast reaction with the monomer.

The monomer recombination reaction is fast but the polymerization reactions (reaction 2) are even faster. This rapid polymerization is the reason that the rate measurement is so difficult for this system.

The current values of the rate constants (eq 33–37) differ somewhat from those of ref 1 (eq 3 and 4). The upper limit for the recombination rate (eq 3) reported in ref 1 is correct for the reaction with small polymeric species. The experimental conditions in ref 1 were such that the dominant recombination reaction was the polymeric reaction. The higher values in this paper (eq 34 and 36–37) for the polymerization reactions (reaction 2) have three possible explanations. First, the fast monomer recombination reaction resulted in an underestimate of the $[UF_5]$ concentration shortly after photolysis in ref 1. This in turn gave a low value of the rate constant. Second, the experimental technique in ref 1 may have been deficient. The technique was to use an infrared diode laser to monitor the reaction of UF_5 monomer. The authors assumed that only the monomer absorbed. This assumption may not have been correct. Third, the precision is low in the current experiments at early times and may have contributed to the differences.

Our value for k_{rm} is two to three times the value estimated[1] from the equilibrium constant and the dissociation rate[12] at 1200 K. Because our experiments were at room temperature, this difference is not necessarily a disagreement. It is very unlikely that the dissociation activation energy is a constant over such a broad temperature range.

The most reliable result of this set of experiments is the rate constant ratio k_{mm}/k_{rm} (eq 23). The individual rate constants are somewhat less accurately determined. The major sources of uncertainty are the low signal-to-noise ratio at early times, uncertainty in the measured pulse energies, window transmittance, and beam area, and the amount of absorption by UF_5. Taking all of these factors into consideration, we estimate that the uncertainty in k_{rm} and k_{mm} is ±60%. The values of k_{rp}, k_{mp}, and k_{pp} have about the same precision, but they depend to some extent on the reliability of the assumption that the reaction rates are proportional to the collision rate.

The dependence of the particle size on the rates of reactions 1 and 2 required that the rate scaled with collision rate (eq 20–22). This assumption may not be valid. We believe, however, that it is the best assumption in absence of additional experimental information.

Our estimate of the collision rate may be low for large clusters. We assumed a close packing of the UF_5 moieties. Voids in the particles would increase the collision cross sections and, hence, the collision rates. If voids are indeed present, they will have only a minor effect on the derived rate constants. For example, the greatest effect of voids would be for the largest clusters. These form at the lowest fluorine fraction (Figure 13). We calculated the effect of adding voids sufficient to double the cluster size on what would be the worst case (no F_2, Figure 6) and found that this large void fraction resulted in only a 20% change in the value (eq 35) of k_{rp}.

The rate of reaction of fluorine atoms with UF_5 polymer (eq 35) was derived from long-time (35 ms) recovery of the probe transmittance (Figures 5–9). Several processes could interfere with this determination. One of these is that any traces of oxygen would produce O_2F by reaction 5. For example, only a 3-ppm O_2 impurity would be necessary to give the observed positive deviation from the prepulse base line in Figure 9. Another possible process is the reaction of photolytic atomic fluorine with any solid residual UF_5. Both of these would increase the apparent UF_6 concentration after the laser pulse. This type of interference would tend to increase the apparent value of k_{rp}.

The monomeric forms of reactions 1 and 2 are both recombination reactions and require a third-body collision for stabilization. The total pressure range in these experiments was not really sufficient for testing the pressure dependence (350 to 1000 Torr), but the experiments do suggest that this pressure range is near the high-pressure limit.

Acknowledgment. This work was sponsored by the Centrifuge Machine Division, Martin Marietta Energy Systems, and the Los Alamos National Laboratory. We appreciate this support. We thank Dr. L. B. Asprey for preparation of the high-purity fluorine and Mr. Fred Archuleta and Mrs. Deanna Seitz for assistance with the experiments.

Registry No. UF_5, 13775-07-0; F, 14762-94-8.

(12) Schug, K. P.; Wagner, H. Gg. *Z. Phys. Chem.* **1977**, *108*, 172.